Thermal Reversible Breakdown and Resistivity Switching in Hafnium Dioxide

M.A. Danilyuk[1], D.B. Migas[1], A.L. Danilyuk[1], V.E. Borisenko[1],
X. Wu[2], N. Raghavan[2], K.L. Pey[2]

[1] *Belarusian State University of Informatics and Radioelectronics, 6, P. Browki Str., 220013 Minsk, Belarus*
[2] *Nanyang Technological University, Nanyang Ave., 639798 Singapore, Singapore*

We present a model of thermal reversible breakdown via conductive filaments (CFs) in hafnium dioxide (HfO_2). These CFs appear as a result of electrical pretreatment of a metal/HfO_2/metal (semiconductor) nanostructure (MIM(S)). The model is based on an assumption that the thermal reversible breakdown of a CF is due to of Joule heating displaying an exponential dependence of conductivity on temperature. The corresponding current-voltage characteristic and temperature of a CF in its middle and at the interface with an electrode are calculated taking into account the heat conduction equation and boundary conditions with heat dissipation via electrodes. It is found that the current-voltage characteristic of a CF has three specific regions. The initial and final regions have turned out to be linear with respect to the current and display different slopes, while the middle region is characterized by both the S-shaped and ultralinear dependences which are affected by the ambient temperature and nanostructure parameters. The switching potential from the high resistivity state (HRS) to the low resistivity state (LRS) was shown to decrease with the ambient temperature and with worsening of heat dissipation conditions.

Keywords: Hafnium dioxide, Thermal reversible breakdown, Conductive filament, S-shaped, Current-voltage characteristic.

1. INTRODUCTION

HfO_2 nanostructures are currently considered to be very promising for different applications including gate oxides in Si transistors and emerging nonvolatile memory cells such as resistive random access memory (RRAM). For RRAM development a clear understanding of switching mechanisms from a HRS to a LRS is demanding. Several models were proposed to explain the switching effect [1-3], however, they did not cover comprehensively experimental observations. It is experimentally shown by means of high resolution transmission electron microscopy that formation of CFs with diameters of 30-50 nm in HfO_2 occurred by an electrical pretreatment [2]. According to experimental data [3,4] current-voltage characteristics of MIM(S) nanostructures with HfO_2 are characterized by a current jump at a specific set voltage (V_{set}) indicating that only the current-voltage characteristic of a CF displays both the S-shaped and ultralinear behavior. In order to provide an interpretation of such behavior we have developed a model of thermal switching breakdown due to the Joule heating of CFs.

2. MODEL

We have assumed a CF to be formed along the z axis from $z = -L/2$ to $z = +L/2$ in a HfO_2 layer of MIM(S) nanostructure The heat release and voltage drop at contacts are not taken into consideration because heat removal is expected to be uniformed and to follow the Newton law. Temperature distribution in the CF can be written as [5]

$$\kappa_d \frac{d^2T}{dz^2} + jF = 0 , \qquad (1)$$

$$\frac{dT}{dz}\bigg|_{z=0} = 0, \quad \kappa_d \frac{dT}{dz}\bigg|_{z=L/2} = \frac{\lambda(T_b - T_0)}{1 + \lambda\delta / \kappa_c} , \qquad (2)$$

where κ_c is the heat conduction of a contact, κ_d is the heat conduction of a CF, λ is the coefficient of external heat removal, δ is the thickness of contacts, T_0 is the ambient temperature, T_b is the temperature at the interface between the CF and the electrode. The current density and the voltage drop on the CF can be defined in a drift approximation

$$j = \sigma_0 F \exp(-\Delta E / k_B T), \quad V = 2\int_0^{L/2} F(z)dz , \qquad (3)$$

where F is the electric field strength in the CF, σ_0 is the conductivity in the CF at T_0, ΔE is the trap energy in the CF, k_B is the Boltzmann constant.

By solving (1)-(3), the current-voltage characteristic of the CF can be calculated in the parametric form

$$j_R = \int_{t_b}^{t_m}\left(\int_t^{t_m} \exp(1/t)dt\right)^{-1/2} dt, \quad \frac{v_b^2}{2} = \int_{t_b}^{t_m} \exp(1/t)dt , \qquad (4)$$

where

$$v_b = (V/2)\sqrt{(\sigma_0 k_B / \kappa_d \Delta E)} , \quad j_R = (\sqrt{2}/4)jL[k_B / (\kappa_d \Delta E \sigma_0)]^{1/2} ,$$

$$t_b = t_0 + (jV/W_b) , \quad W_b = (4\gamma\kappa_d\Delta E)/(k_B L) , \quad \gamma = \lambda L / 2\kappa_d[1 + (\lambda\delta / \kappa_c)] ,$$

$$t_{(0,m)} = k_B T_{(0,m)} / \Delta E , \quad T_m \text{ is the temperature in the middle of the CF at } z = 0.$$

$$\left(\int_{t_0+jV/W_b}^{t_m} \exp\left(\frac{1}{t}\right)dt\right)^{1/2} \cdot \int_{t_0+jV/W_b}^{t_m}\left(\int_t^{t_m} \exp\left(\frac{1}{t}\right)dt\right)^{-1/2} dt - $$
$$- \frac{jV}{W_b}\frac{\gamma}{2} = 0. \qquad (5)$$

We have defined the function $t_m(jV/W_b)$ at different values of γ and t_0 parameters and, as a consequence, find the current-voltage characteristics and temperature dependencies in the middle of a CF and at the interface with electrodes on voltage drop.

3. RESULTS AND DISCUSSION

We have found three specific regions in the current-voltage characteristic of a CF. The first region at a small voltage drop is characterized by a linear dependence of current density with a small slope. The slope is found to be slightly dependent on temperature t_0 and independent of the parameter of heat removal γ. The second region is a transition state which displays the nonlinear current voltage characteristic depending on t_0 and γ. This region is S-shaped with the following transformation to nonlinear transition area with increasing t_0. Finally the third region shows the linear current-voltage characteristic with a high slope and obeys the Ohm law. The shape of the current-voltage characteristic is only defined by t_0 and γ. At $t_0 \leq 0.3$ between the linear regions the S-shaped region appears while at $t_0 > 0.35$ there is a nonlinear area. The current-voltage characteristic shifts along the voltage drop axis with increasing the heat removal parameter γ and the formation the S-shaped regions occurs at larger voltage drops as shown in Fig. 1.
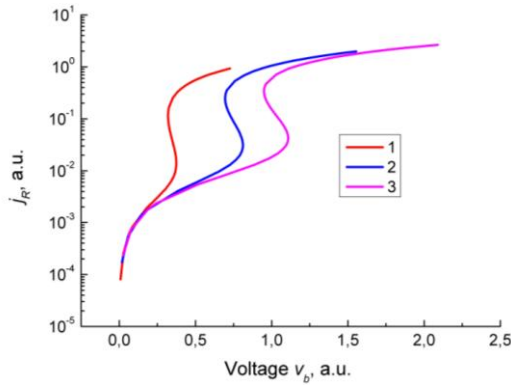

Fig. 1 – Current-voltage characteristics of the CF at $t_0 = 0.2$: $\gamma = 0.1$ (1); $\gamma = 1.0$ (2); $\gamma = 0.5$ (3)
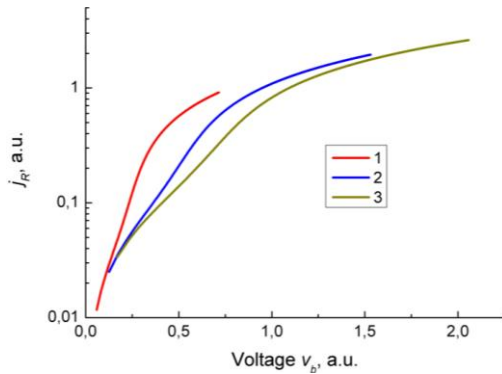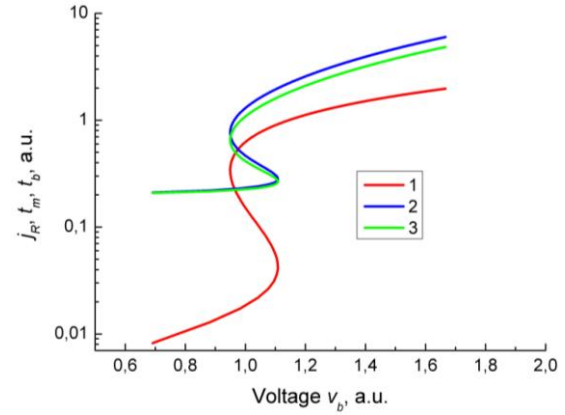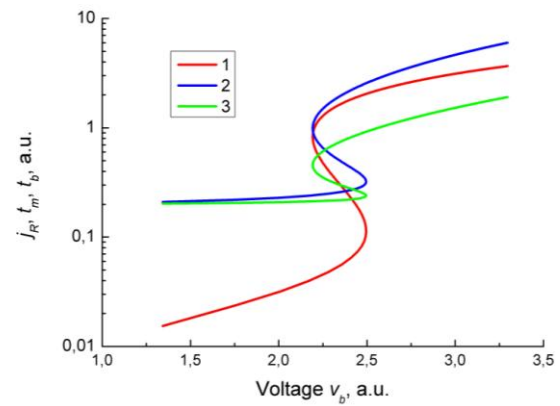

Fig. 2 – Current-voltage characteristics of the CF at $t_0 = 0.5$: $\gamma = 0.1$ (1); $\gamma = 0.5$ (2); $\gamma = 1.0$ (3)
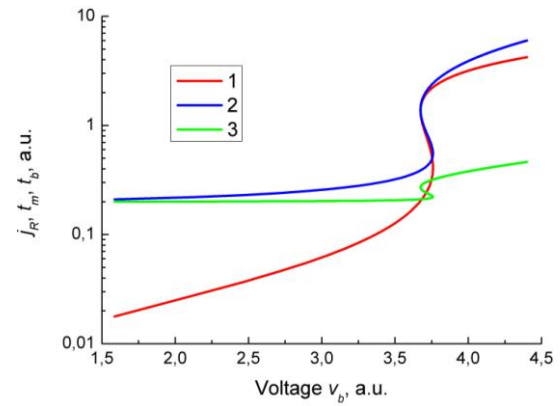
At $t_0 = 0.5$ the current-voltage characteristic becomes more flattened and the S-shaped area practically disappears. Instead, it is characterized by a smaller slope. The middle part of the current – voltage characteristic shifts in the region of the higher external bias with increasing the heat removal parameter γ. In other words, the temperature dependence is characterized by the disappearance of the S-shaped region and the decrease of the slope.

Fig. 3 – Current-voltage characteristics of the CF (1), temperatures t_m (2) and t_b (3) at $t_0 = 0.2$: a) $\gamma = 1$; b) $\gamma = 10$; c) $\gamma = 100$

It is evident from Fig. 3 that the region of S-shaped current – voltage characteristic shifts towards larger external bias as well as larger current with increasing the heat removal parameter. The temperature dependence in the middle of dielectric also shifts towards larger external bias. In other words, the S-shaped region occurs at the higher external bias.

The S-shaped area of the temperature dependence in the middle of nanostructure moves slightly upwards along the temperature axis with heat removal parameter, while remaining almost unchanged in size.

Whereas, the interface temperature behaves differently. When $\gamma = 1$, interface temperature is almost equal to a temperature in the middle of dielectric.

When $\gamma = 10$ the difference between these temperatures becomes significant, especially in the S-shaped region. Herewith, the S-shaped dependence of ambient temperature preserves, but shrinks along the temperature axis. When $\gamma = 100$ this difference is significantly increased and the ambient temperature dependence is strongly compressed along the temperature axis. Thus, with increasing of the heat removal parameter temperature at the interface is significantly reduced compared with temperature at the center of insulator. The difference between these temperatures is also increasing with the increasing of the external bias. Temperature T_b does not differ from T_0 in the region of increasing of internal bias until the formation of the S-shaped area.

Increasing the temperature t_0 at the constant heat removal parameter γ leads to an increase of the S-shaped area along the voltage axis. Moreover, only the lower part of this area is affected, while the upper part (a range of currents $j_R = 0.1\text{-}1.0$) does not depend on t_0, as it is shown in Fig. 4.

This is important to obtain the necessary switching potential: with increasing of ambient temperature t_0 the S-shaped area narrows and switching potential decreases.
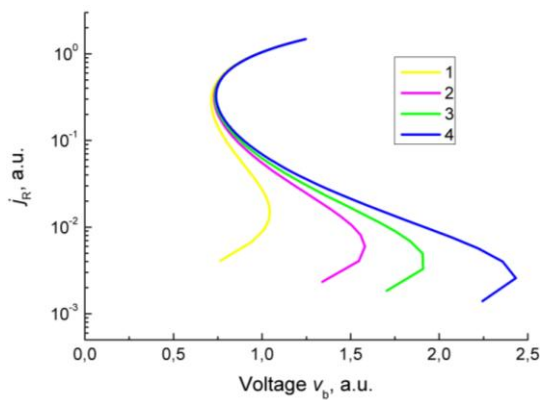

Fig. 4 – Current-voltage characteristics of the CF beyond ambient temperatures: $\gamma = 0.5$; $t_0 = 0.17$ (1), $t_0 = 0.14$ (2), $t_0 = 0.13$ (3), $t_0 = 0.12$ (4)

The temperature of CF dependences on the voltage drop are also characterized by three regions, as it is sown in Fig. 3, 5. We have also found that the influence of parameters of a nanostructure on this dependence is analogues to the one described above for the current-voltage characteristic. A notable difference can be traced for temperature only at the boundary of a CF. At $\gamma \leq 1$ the temperature corresponds to that in the middle of the CF. Whereas, with increasing γ the difference has turned out to be valuable leading to compression of the $T_b(v_b)$ dependence with respect to the temperature

axis. Thus, with increasing of the heat removal the temperature of the CF at the boundary decreases significantly with respect to the temperature in the middle of the CF.
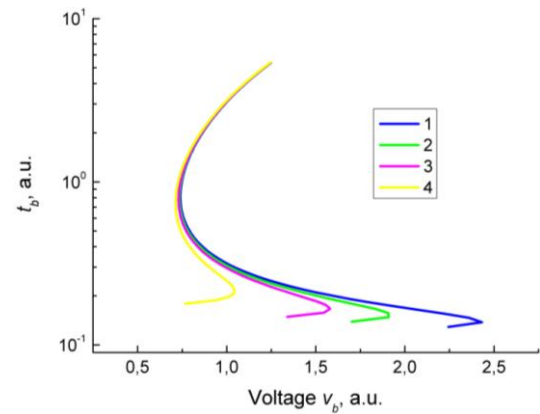

Fig. 5 – Interface temperature beyond ambient temperatures: $\gamma = 0.5$; $t_0 = 0.12$ (1), $t_0 = 0.13$ (2), $t_0 = 0.14$ (3), $t_0 = 0.17$ (4)

The potential, at which a sharp jump in the current occurs (the switching potential from HRS to LRS, V_{set}), decreases proportionally to increasing of the ambient temperature T_0 according to experimental data [4] for the Pt/HfO$_2$/TiN nanostructure. The potential V_{set} also decreases proportionally to the parameter γ because of the worsened conditions of heat removal.

4. CONCLUSIONS

We have developed the model of conductive filament thermal reversible breakdown involving mechanisms of switching between high and low resistivity states in HfO$_2$ MIM(S) nanostructures. The current-voltage characteristics and dependencies of the filament temperature on the voltage drop, ambient temperature and heat removal parameters are also calculated. We have defined conditions of an appearance of the S-shaped current-voltage characteristic of the conductive filament with a nonlinear transition area. We have also found out that decreasing in the ambient temperature leads to magnification of the transition S-shaped region of the current-voltage characteristic while degeneration of this transition region occurs with an increasing temperatute. An increase in the heat removal shifts the current-voltage characteristic to the area of larger voltage drops and decreases the temperature at the filament/electrode interface with respect to the temperature at the middle of the conductive filament.

REFERENCES

1. P. Gonon, M. Mougenot, et al., *J. Appl. Phys.* **107**, 074507 (2010).
2. X. Li, K.L. Pey, et al., *Appl. Phys. Lett.* **96**, 022903 (2010).
3. X. Wu, K.L. Pey, et al., *Appl. Phys. Lett.* **96**, 202903 (2010).
4. Z. Fang, H.Y. Yu, et al., *IEEE Electr. Device L.* **31**, 476 (2010).
5. K.D. Tsendin, A.B. Shmelkin, *Tech. Phys. Lett.* **30**, 525 (2004).